Sensors & Actuators: B. Chemical 282 (2019) 366–372

Contents lists available at ScienceDirect

Sensors and Actuators B: Chemical

journal homepage: www.elsevier.com/locate/snb

Sensitive fluorescence sensor for point-of-care detection of trypsin using glutathione-stabilized gold nanoclusters

Hongxia Li[a], Mingming Yang[b], Deshuai Kong[a], Rui Jin[a], Xu Zhao[a], Fangmeng Liu[a], Xu Yan[a,*], Yuehe Lin[c,*], Geyu Lu[a,*]

[a] State Key Laboratory on Integrated Optoelectronics, College of Electronic Science and Engineering, Jilin University, 2699 Qianjin Street, Changchun, 130012, China
[b] College of Plant Protection, Nanjing Agricultural University, Nanjing, Jiangsu Province, 210095, China
[c] School of Mechanical and Materials Engineering, Washington State University, Pullman, WA, 99164, United States

ARTICLE INFO

Keywords:
Fluorescence
Gold nanoclusters
Electron transfer
Trypsin
Test strips

ABSTRACT

There is an urgent demand for on-site detection of biomarker, particularly in clinical diagnosis and therapeutics applications. Herein, we designed a convenient and sensitive fluorescence nanosensor for point-of-care determination of trypsin (TRY). The fluorescence intensity of gold nanoclusters (AuNCs) can be quenched by cytochrome c (Cyt c) via electron transfer mechanism. TRY specifically catalyzes the hydrolysis of Cyt c to produce small peptide fragments, inducing the significant fluorescence recovery. As a result, the AuNCs-based system processed a sensitive and selective response to TRY with the range 0.2–100 μg mL^{-1}, accompanying a detection limit of 0.08 μg mL^{-1}. Significantly, the sensing assay can be used to construct test strips for rapid and visual recognition of TRY. Combining with smartphone and ImageJ software, we further developed an image processing algorithm for quantitative detection of TRY with highly promising, which validated the potential point-of-care application.

1. Introduction

Considerable efforts have been made for the design of analytical strategies toward biological macromolecules in order to diagnosis and treatment of disease [1]. Trypsin (TRY) as an important serine protease can catalyze the hydrolysis of some proteins into small pieces [2,3]. The enzyme that can regulate pancreatic exocrine function served as a reliable and specific biomarker for pancreatitis [4]. Abnormal level of TRY (0.60–6.55 μg mL^{-1}) can cause cystic fibrosis [5], pancreatic carcinoma [6] and meconium ileus [7]. Therefore, the sensitive analysis of TRY is important for efficient diagnosis and therapeutics of diseases, as well as applications in the proteomics area. Vast endeavors have been undertaken to identify and quantify TRY, including high-performance liquid chromatography [8], enzyme-linked immunosorbent assay [9], electrochemical methods [10] and fluorescence spectroscopy [11]. Among them, fluorescence (FL) strategy as one of the most powerful sensing platforms have received considerable attention due to its characteristics of simplicity, rapid, sensitivity and cost-effective. To date, few FL strategies have also been developed for the detection of TRY based on fluorescent dyes [12,13], quantum dots [14] and graphene quantum dots [15]. However, most of nanomaterials suffer from the biological toxicity or complex fabrication procedure, which limited their wide application in biological system. Thus, it still remains great challenge to develop facile and sensitive strategy for the determination of TRY.

Recently, fluorescent noble gold nanoclusters (AuNCs) as an excellent candidate have attracted significant interest due to their superior optical properties as well as facile synthetic process [16]. Compared to organic dyes and quantum dots, AuNCs possess distinct advantages, such as preferable biocompatibility, excellent photostability and low toxicity [17]. Particularly, one-step green synthesis of AuNCs [18] without the requirement of toxic organic solvents and reducing agent makes them attractive and in-depth development. Benefiting from these characteristics, AuNCs have been widely applied in the construction of biosensors for the detection of metal cations [19], inorganic anions [20], small biomolecule [21–23] and industrial chemical [24]. Instead, the AuNCs-based FL sensing platform for enzyme activity detection is still in its starting so far. Thus, the utilization of AuNCs for the monitoring of enzyme activity have exhibited great prospects, since both the excellent optical characters and outstanding selectivity have been effectively combined.

Inspired by the aforementioned facts, we herein designed a facile AuNCs-based sensing platform for the sensitive detection of TRY (Scheme 1). Employing a convenient one-pot synthetic route, AuNCs were

* Corresponding authors.
E-mail addresses: yanx@jlu.edu.cn (X. Yan), yuehe.lin@wsu.edu (Y. Lin), lugy@jlu.edu.cn (G. Lu).

https://doi.org/10.1016/j.snb.2018.11.077
Received 29 July 2018; Received in revised form 24 October 2018; Accepted 15 November 2018
Available online 16 November 2018

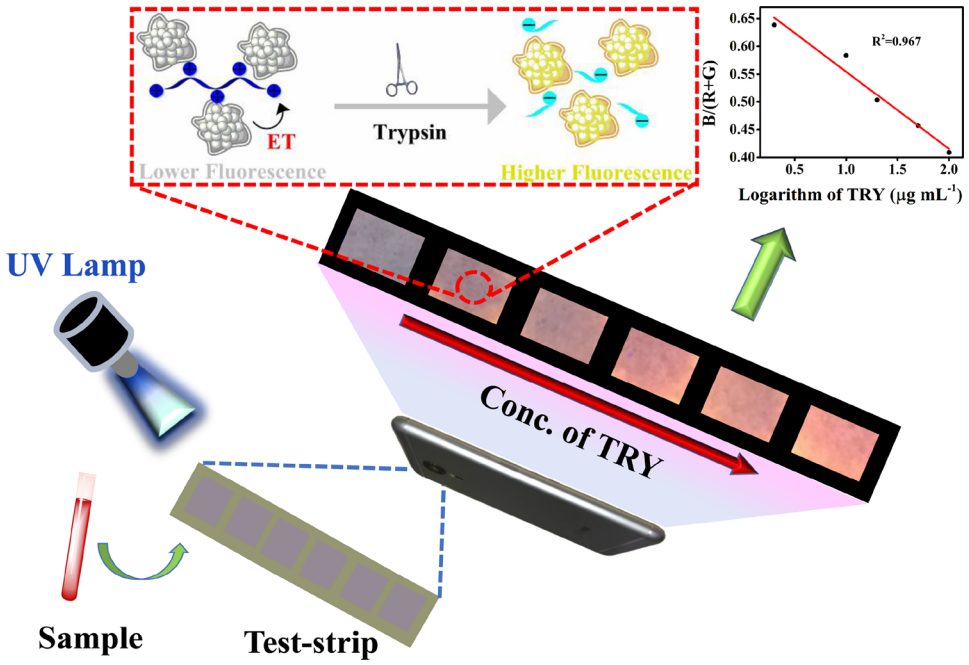

Scheme 1. Schematic illustration of the principles of detection TRY.

synthesized by using glutathione (GSH) as template and stabilizer. The positively charged cytochrome c (Cyt c) can efficiently couple to oppositely charged AuNCs, resulting in obvious FL quenching through electron transfer (ET) mechanism. TRY can specifically hydrolyze Cyt c to yield negatively charged heme-peptide fragments, weakening the ET effect, which induced the recovery of FL intensity. On the basis of the FL quenching induced by Cyt c and following recovery in the presence of enzyme, this facile and label-free strategy performed high sensitivity for TRY detection. More importantly, AuNCs have also been applied to construct portable test strips for rapid and visual detection of TRY, implying that this sensor has promising potential for point-of-care monitoring.

2. Experimental

2.1. Reagents and materials

The water with good resistivity (> 18 MΩ cm^{-1}) were utilized in this work. Hydrogen tetrachloroaurate (III) hydrate ($HAuCl_4 \cdot xH_2O$), L-glutathione, TRY (180 U mg^{-1}), ascorbic acid, lactose, glucose, tyrosine, aspartic acid, glycine, BSA (bovine serum albumin), ConA (concanavalin A), GoX (glucose oxidase), acetylcholinesterase (AChE), butyrylcholinesterase (BChE) of analytical grade were obtained from Sigma-Aldrich Corporation.

2.2. Preparation of AuNCs

GSH capped AuNCs were synthesized based on the previous process [25]. In brief, 0.5 mL of $HAuCl_4$ (20 mmol L^{-1}) and 0.15 mL of GSH (100 mmol L^{-1}) were mixed and added to 4.35 mL of ultrapure water under vigorous stirring. Then, the above mixture was heated to 70 °C and reaction was allowed to proceed for 24 h. Thus, a yellow solution of AuNCs was obtained and purified by use of dialysis bag (3 kDa). The concentration of AuNCs was 1.75 mmol L^{-1} (calculated by the concentration of Au).

2.3. Fluorescence quenching experiments induced by Cyt c

Various concentrations of Cyt c (0–500 μg mL^{-1}) and 50 μL of AuNCs (0.5 mmol L^{-1}) and were introduced into 500 μL calibrated test tubes. The tubes were diluted to mark by using pH = 8.0 PBS solution (10.0 mmol L^{-1}). The FL spectrum were measured by using spectrofluorophotometer with excitation wavelength at 418 nm.

2.4. Detection procedure for TRY activity

200 μg mL^{-1} of Cyt c (50 μL) and 10 mmol L^{-1} of PBS (pH = 8.0, 50 μL) were mixed with various concentrations of TRY (50 μL) for 60 min at 37 °C. Then, 0.5 mmol L^{-1} of AuNCs (50 μL) were added and diluted to 500 μL with PBS (pH = 8.0, 10.0 mmol L^{-1}). The FL spectra of mixture were collected with excitation wavelength at 418 nm.

2.5. TRY detection in biological samples

The fresh human blood samples were collected from Changchun China Japan Union Hospital. The serum samples were centrifuged at 10,000 rpm for 5.0 min at 4 °C. Then, the supernatants were diluted 50-fold with PBS (pH = 8.0, 10.0 mmol L^{-1}) before detection. For urine samples analysis, the urine samples were diluted 50-fold with PBS for analysis.

3. Results and discussion

3.1. Characterization of AuNCs

GSH-capped AuNCs were synthesized through a convenient one-pot synthetic method in water phase [25]. The morphology of as-prepared AuNCs was directly observed by using transmission electron microscopy (TEM). As displayed in Fig. 1A, the AuNCs were mostly spherical morphology with good dispersion and existed average diameter size around 2.7 nm. The optical properties of AuNCs were confirmed by UV–vis and FL spectroscopy. As shown in Fig. 1B, AuNCs had no apparent absorption in the visible region, implying that the diameter of AuNCs was less than 10 nm. The typical excitation and emission wavelengths of AuNCs were 418 nm and 625 nm, respectively. The large stokes shift of 200 nm can efficiently avoid interference between the excitation and emission signals. Inset in Fig. 1B showed the color of AuNCs solution under visible light (light yellow) and UV light (orange). These results confirmed that the successful preparation of AuNCs can be used for fabrication biosensor.

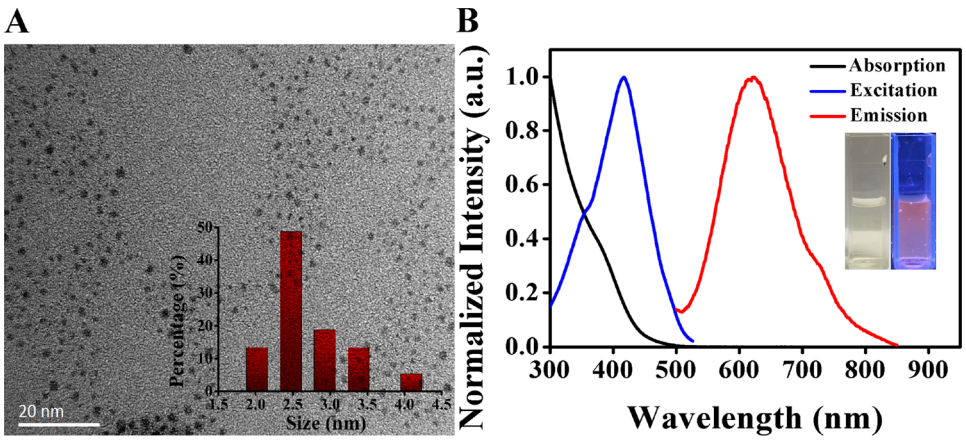

Fig. 1. (A) Typical TEM image of AuNCs. (B) The UV–vis absorption (black line), fluorescence excitation (blue line) and emission (red line) spectra of AuNCs. (Inset) Digital photos of AuNCs under visible light (left) and UV light (right). (For interpretation of the references to colour in this figure legend, the reader is referred to the web version of this article).

3.2. Design of AuNCs-Cyt c platform

In order to design a sensitive system for the determination of TRY, the AuNCs-based sensing platform coupled with the specificity of enzyme was developed. The FL intensity of AuNCs at 625 nm can be significantly quenched by Cyt c through ET process (Fig. 2A, Red line). Under catalysis of TRY, Cyt c was hydrolyzed into negatively charged heme-peptide fragments [26,27], resulting in the weak ET effect and the FL recovery of system (Blue line). The emission color of reaction samples under UV lamp (365 nm) can be observed visually, which coincide with the variation of FL intensity (Inset, Fig. 1A). To verify the feasibility of the designed platform for TRY, control experiment in absence of Cyt c were studied in Fig. S1. It can be obviously found that the FL of AuNCs cannot be influenced by TRY in wide range from 0 to 100 μg mL^{-1}. All of the above results indicated that the designed AuNCs-Cyt c platform can be applied to analyze TRY.

Cyt c as a popular electron transfer substance can efficiently quench the FL intensity of fluorophore [26]. For better explore the quenching process induced by Cyt c, relevant studies were carried out. The zeta potential of AuNCs and Cyt c were investigated in Fig. 2B. The AuNCs were negatively charged ($\zeta = -24.18$ mV) while the Cyt c were positively charged ($\zeta = +17.99$ mV), indicating that the strong electrostatic interaction between AuNCs and Cyt c. Furthermore, the electrostatic interaction would result in slight aggregation of AuNCs (Fig. 2C), which was also clearly observed by TEM (Fig. 2D). Most importantly, the FL lifetime of AuNCs (8.172 μs) was appreciably shortened in the presence of dynamic quencher (here heme in Cyt c), revealing that dynamic quenching process was dominant for FL decrease (Fig. 2E and Table S1). The designed mechanism was that the positive charge of Cyt c can accept the electron from AuNCs, and then deliver them from the lowest unoccupied molecule orbital (LUMO) to the highest occupied molecule orbital (HOMO). Thus, the strong electrostatic interaction between AuNCs and Cyt c make them closer, further causing electron transfer from AuNCs (donor) to Cyt c (accepter), which induced FL dynamic quenching. We systematically investigated the FL quenching of AuNCs in the presence of Cyt c. As depict in Fig. 2F, the FL intensity (625 nm) were gradually quenched with the increasing concentration of Cyt c (0–500 μg mL^{-1}). There is a good linear relationship between F_Q/F_{Q0} and the logarithm of Cyt c concentration ($R^2 = 0.9947$). F_Q and F_{Q0} are FL intensities in the presence and absence of Cyt c, respectively. The regression equation is $F_Q/F_{Q0} = 1.3233\text{-}0.5105 \log [\text{Cyt c}]$. To obtain low background and high sensitivity, 20 μg mL^{-1} of Cyt c was chosen for further study.

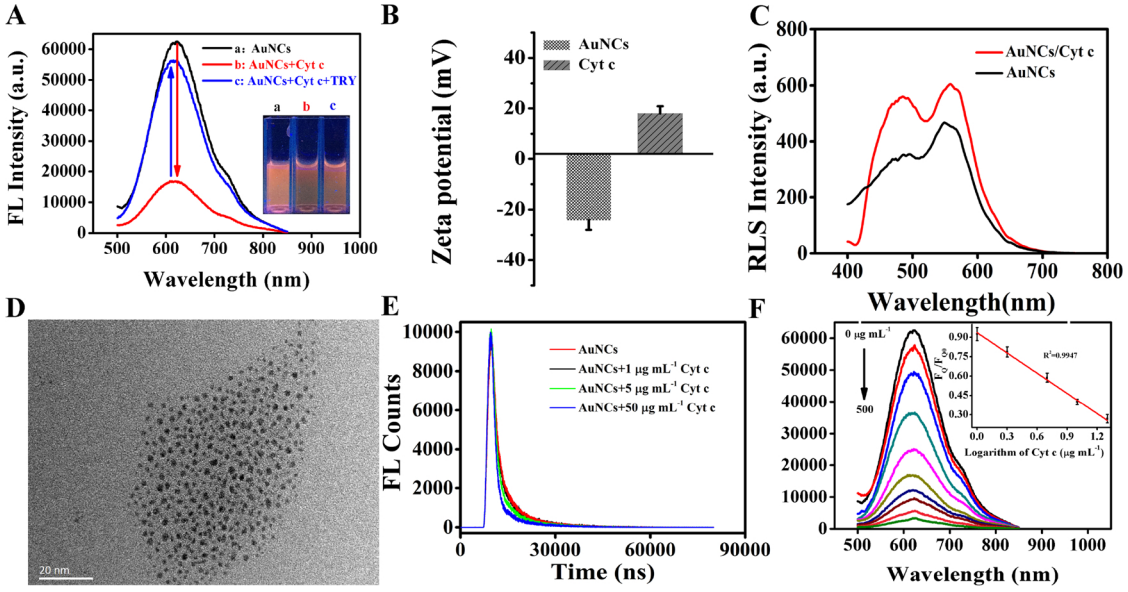

Fig. 2. (A) Fluorescence spectra of AuNCs, AuNCs-Cyt c and AuNCs-Cyt c-TRY. The final concentration of Cyt c and TRY are 20 and 100 μg mL^{-1}. Inset are the corresponding color changes of AuNCs (a), AuNCs-Cyt c (b) and AuNCs-Cyt c-TRY (c) under UV light. (B) The zeta potentials of AuNCs and Cyt c at pH 8.0. (C) TEM image of AuNCs-Cyt c. (E) The resonance light scattering (RLS) spectra of AuNCs and AuNCs-Cyt c. (F) FL spectra of AuNCs in the presence of different concentrations of Cyt c. The concentration of Cyt c are 0, 1.0, 2.0, 5.0, 10, 20, 50, 100, 200 and 500 μg mL^{-1}. Inset are the linear plot of the FL intensity ratio F_Q/F_{Q0} versus the logarithm of Cyt c concentration.

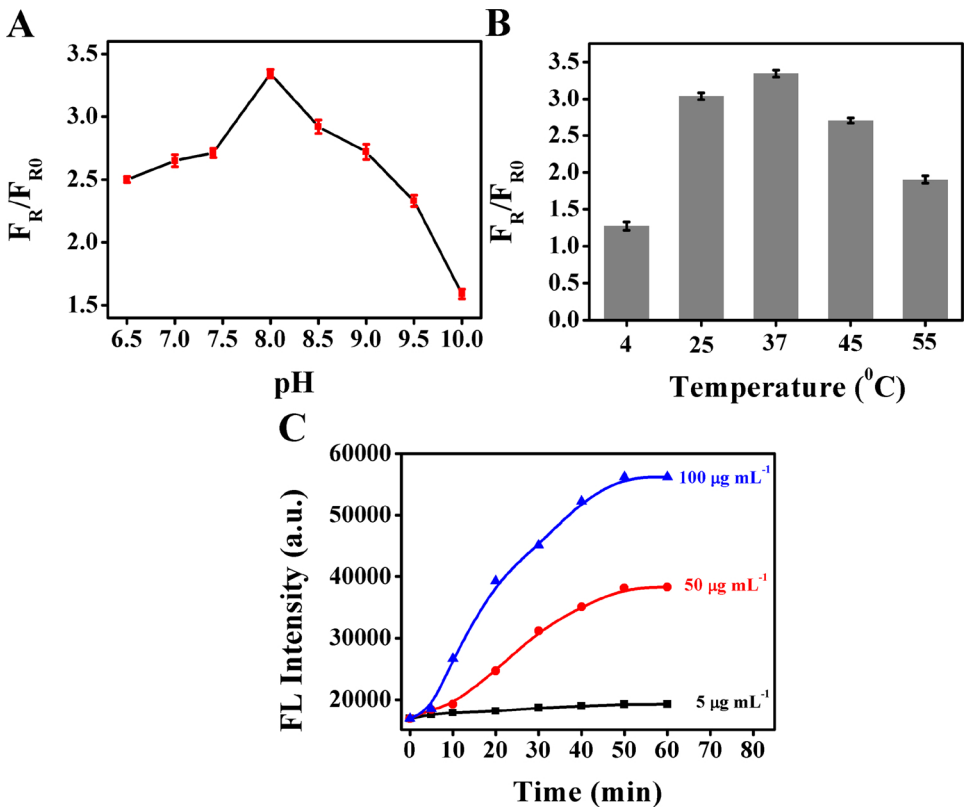

Fig. 3. The effect of pH (A) and reaction temperature (B) on the FL intensity ratio F_R/F_{R0}. (C) The effect of time on F_R/F_{R0} of the AuNCs-Cyt c system in the presence of 5.0, 50 and 100 μg mL^{-1} TRY. The final concentration of Cyt c is 20 μg mL^{-1}.

3.3. Optimization of experimental conditions

To achieve a good performance for TRY detection, the experimental conditions (e.g. pH, incubation temperature and reaction time) were optimized in our studies. The effect of pH on the FL ratio (F_R/F_{R0}) of AuNCs-Cyt c system in the presence of 100 μg mL^{-1} TRY was investigated (Fig. 3A). F_R and F_{R0} are FL intensities of AuNCs-Cyt c system in the presence and absence of TRY, respectively. The F_R/F_{R0} obviously increased with the pH value from 6.5 to 8.0, following by apparently decreasing in pH range of 8.5–10.0. It could be seen that the hydrolysis ability of TRY performed good in alkaline medium (pH = 8.0). However, the catalytic activity of TRY could be damaged at higher pH value, causing the decrease of F_R/F_{R0}. Therefore, pH 8.0 PBS (10 mmol L^{-1}) was chosen for TRY activity detection.

Reaction temperature was optimized by measuring the F_R/F_{R0} of AuNCs-Cyt c system. As displayed in Fig. 3B, F_R/F_{R0} reached the maximum at 37 °C, which was consistent with previous study [27,28]. Thus, 37 °C was selected for TRY activity detection. The catalytic reactions time were consecutively monitored by FL spectroscopy in the presence of TRY (5.0, 50 and 100 μg mL^{-1}) at 37 °C. It can be seen from Fig. 3C that the reaction time had remarkable influence on the FL intensity. When TRY was introduced into the AuNCs-Cyt c system, the FL intensity gradually enhanced and completed within 60 min, confirming that 60 min was chosen for TRY detection. Under optimized condition, the AuNCs-Cyt c system possessed good stability in a wide salt concentration (0–50 mmol L^{-1}), implying that this system was expected to fabricate biosensor for TRY (Fig. S2).

3.4. Detection of TRY activity

The determination of TRY activity with the AuNCs-Cyt c system was conducted under the optimum conditions, the FL intensity of AuNCs-Cyt c system was continuously recovered with the increasing of TRY concentration, depict in Fig. 4A. Inset showed the change trend of FL intensity in the presence of various concentrations of TRY. There is a good linear relationship (R^2 = 0.9916) between the FL intensity ratio F_R/F_{R0} of AuNCs-Cyt c platform and TRY concentration in the range of 0.2–100 μg mL^{-1} (Fig. 4B). F_R and F_{R0} are FL intensities of AuNCs-Cyt c system in the presence and absence of TRY, respectively. The regression equation was: F_R/F_{R0} = 1.0255 + 0.0240 [TRY]. The limit of detection (LOD) was calculated to be 0.08 μg mL^{-1} (3σ/s) [29], which is comparable to or even better than those of reported methods (Table S2). Furthermore, according to previous literature [30], chronic and acute pancreatitis patients have high TRY concentrations between 0.60–6.55 μg mL^{-1} in serum, implying that the proposed platform can meet the detection requirement.

The specificity of the established assay was further investigated by using common interfering substances, including Na^+, K^+, Mg^{2+}, ascorbic acid, lactose, glucose, tyrosine, aspartic acid, glycine, BSA (bovine serum albumin), ConA (concanavalin A), GoX (glucose oxidase), acetylcholinesterase (AChE) and butyrylcholinesterase (BChE). As displayed in Fig. 4C, after the addition of 50 μg mL^{-1} of the above common substances, the FL intensity of the AuNCs-Cyt c system remained nearly constant, indicating that the common substances do not have evident interference on AuNCs-Cyt c platform. The signal response of system performed obvious increase in the presence of 50 μg mL^{-1} TRY, which demonstrated the excellent selectivity to TRY. We then measured the FL of AuNCs-Cyt c system to 50 μg mL^{-1} TRY in the presence of foreign substances. As revealed in Fig. 4D, the sensing system still work the same with foreign substances. The results illustrated that the system exhibited acceptable ability for resisting interference from common coexisting substances. Thus, the proposed biosensor performed good selectivity for TRY monitoring.

To investigate the accuracy of AuNCs-Cyt c platform, the established FL platform was applied for TRY activity detection in biological samples. The average recovery test was measured by utilizing the standard

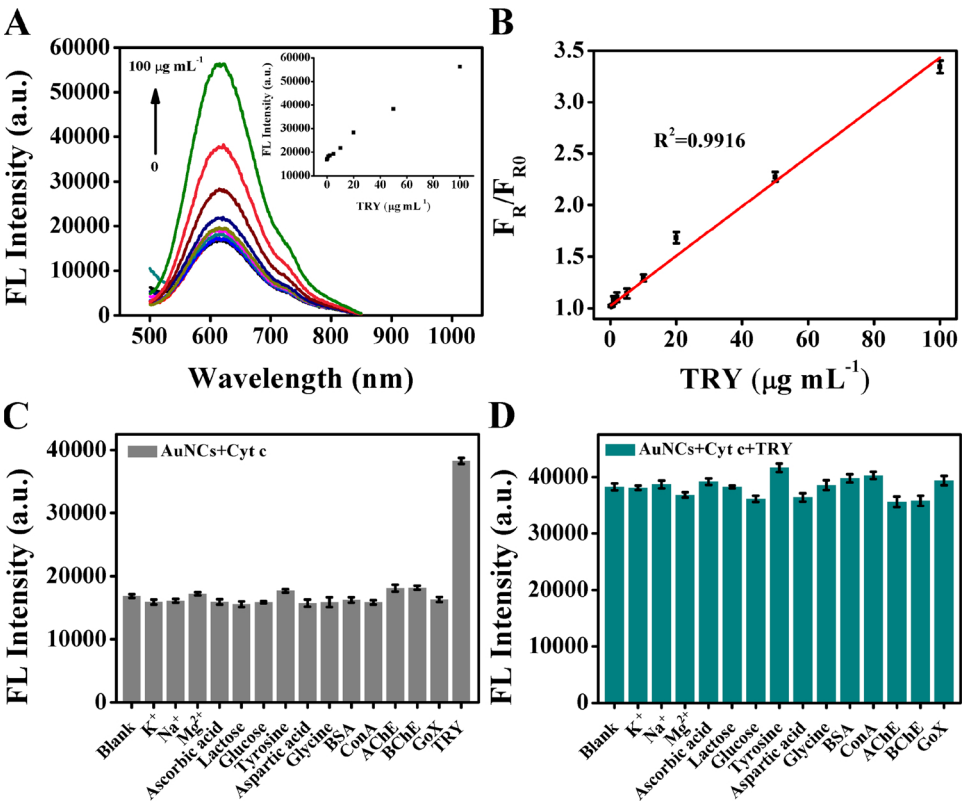

Fig. 4. (A) FL spectra of AuNCs-Cyt c sensing probe with diff ;erent concentrations of TRY. Inset are the change trend of FL intensity with diff ;erent TRY concentrations. The concentrations of TRY were 0.2, 0.5, 1.0, 2.0, 5.0, 10.0, 20.0, 50.0 and 100.0 μg mL^{-1}. (B) Relationship between FL intensity ratio and the concentration of TRY. (C) The FL intensity of AuNCs-Cyt c system in the presence of the interfering substances or TRY (50 μg mL^{-1}). (E) The FL intensity of the AuNCs-Cyt c-TRY system in the presence of the interfering substances (50 μg mL^{-1}).

addition method. Different concentration of standard TRY solution (10, 50 and 100 μg mL^{-1}) were added in the biological sample for recovery test (Table 1). It can be obviously observed that the average recoveries of TRY were in the range from 95% to 109% with low relative standard deviations (RSD < 4.06%). The above results indicated the potential practical application of AuNCs-Cyt c-based platform for TRY analysis in real samples.

3.5. Test strips for TRY detection

Although optical assays have been employed for TRY determination, nearly all optical strategies involve the utilization of bulky spectroscopic instrumentation. From the previous studies, AuNCs had been loaded on various supports, such as glass slide [31] and fibers [32,33], confirming the stability of AuNCs in supports matrices. Inspired by the above facts, we proceeded to establish paper-based sensors by immobilization of AuNCs on common absorbent paper. Paper-based strip as promising platform have received much attention to revolutionize on-site diagnosis due to their low-cost, ease of storage and ease of disposal [34–38]. By prior immobilization of AuNCs on an absorbent paper, test strips were simply designed. Test strips possessed good stability under irradiating continuously over a period of 20 min (Fig. S3). Using the AuNCs-based test paper, we were able to visually detect TRY activity. For TRY detection, 10 μL of the reaction solution (containing TRY and Cyt c) was dropped on the as-fabricated test strip. The color of the paper changed from gray to orange under UV excitation by varying the TRY concentration from 0 to 100 μg mL^{-1} (Fig. 5A). As is known to all, the true-color image can be decomposed by the RGB model into three primary color images. The primary color images can be digitized by ImageJ software, which yielded corresponding intensity values that are related to TRY activity. Based on the above principle, the FL images were taken by a smartphone with high-quality camera, then the images were decomposed into color intensity values of red (R), green (G), and blue (B) channel (Fig. 5B). It can be clearly found that the red (R) channel processed huge enhance in color intensity values and the green (G) channel displayed slight increased with the increase of TRY, while blue (B) channel nearly showed no change in the range of 0–100 μg mL^{-1} TRY, indicating that red (R) channel and green (G) channel images with analyte-dependent intensities. By utilizing image processing algorithm, a linear relationship (R^2 = 0.967) between the B/(R + G) value and the logarithm of TRY concentration in the range of 1–100 μg mL^{-1} was fitted in Fig. 5C. These results demonstrated that the test strips combined with the smartphone offered a highly powerful portable platform for TRY detection due to their cost-effective, simple operation and ease-transport.

Table 1
Detection of TRY in biological samples.

Sample	Spiked concentration (μg mL^{-1})	Found (μg mL^{-1})	Recovery (%)	RSD (n = 3, %)
Urine	10	10.9	109	3.54
	50	49.5	98.9	2.66
	100	102.5	102.5	3.14
Serum	10	10.4	103.7	4.06
	50	49.0	98.1	3.77
	100	95.0	95.0	3.61

4. Conclusions

In the present study, a sensitive FL sensing platform had been established for point-of-care detection of TRY activity by taking advantage of the superior optical properties of GSH-capped AuNCs and excellent specificity of TRY. Initially, the FL intensity of AuNCs could be quenched by positively charged Cyt c through ET mechanism. Then, Cyt c was selectively reduced to heme-peptide fragments by TRY, accompanying the subsequent FL recovery of AuNCs. The practical application of AuNCs-Cyt c system was demonstrated by the analysis of the biological samples with satisfactory results. Meanwhile, the AuNCs-based FL platform were successfully performed on test strips for visual detection of TRY, which validated the potential point-of-care application. Thus,

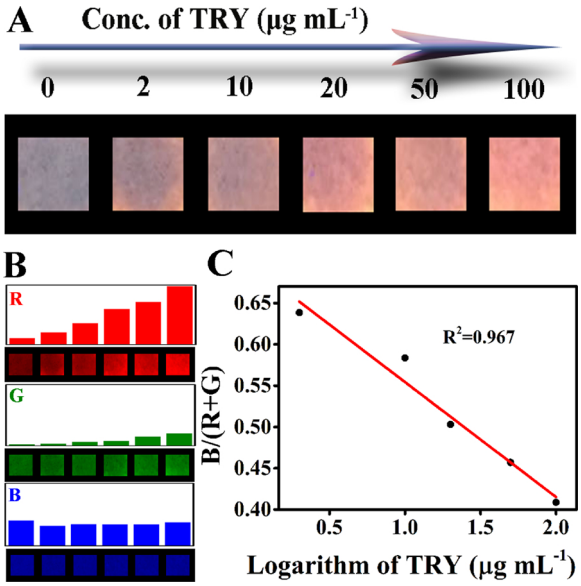

Fig. 5. (A) Visual detection of TRY by using test strips under a 365 nm UV illumination. The concentrations of TRY were 0, 2.0, 10, 20, 50 and 100 μg mL^{-1}, respectively. (B) Intensities of red (R), green (G), and blue (B) channel images of photo images. (C) Relationship between channel intensity ratio and the concentration of TRY. (For interpretation of the references to colour in this figure legend, the reader is referred to the web version of this article).

the platform displayed many merits including ease-of-use, environmental-friendliness, and cost-effectiveness, suggesting that the label-free assay could employ as a promising platform for TRY monitoring.

Conflict of interest

The authors declare no competing financial interest.

Acknowledgements

This work is supported by Science and Technology Development Program of Jilin Province (No. 20170520162JH), the National Key Research and Development Program of China (No. 2016YFC0207300), National Nature Science Foundation of China (21806051), National High-Tech Research and Development Program of China (No. 2014AA06A505), Program for JLU Science and Technology Innovative Research Team (JLUSTIRT 2017TD-07), the Fundamental Research Funds for the Central Universities, China Postdoctoral Science Foundation funded project (No. 2018M631862 and 2017M621199). X. Yan is thankful for support from the National Postdoctoral Program for Innovative Talents (BX201700096).

Appendix A. Supplementary data

Supplementary material related to this article can be found, in the online version, at doi:https://doi.org/10.1016/j.snb.2018.11.077.

References

[1] L.F. Zhang, J.X. Du, A sensitive and label-free trypsin colorimetric sensor with cytochrome c as a substrate, Biosens. Bioelectron. 79 (2016) 347–352.
[2] D. Zhao, C. Chen, J. Zhao, J. Sun, X. Yang, Label-free fluorescence turn-on strategy for trypsin activity based on thiolate-protected gold nanoclusters with bovine serum albumin as the substrate, Sens. Actuators B 247 (2017) 392–399.
[3] L.J. Ou, X.Y. Li, L.J. Li, H.W. Liu, A.M. Sun, K.J. Liu, A sensitive assay for trypsin using poly (thymine)-templated copper nanoparticles as fluorescent probes, Analyst 140 (2015) 1871–1875.
[4] M. Hirota, M. Ohmuraya, H. Baba, The role of trypsin, trypsin inhibitor, and trypsin receptor in the onset and aggravation of pancreatitis, J. Gastroenterol. 41 (2006) 832–836.
[5] A.F. Heeley, D.G. Fagan, Trisomy 18, cystic fibrosis, and blood immunoreactive trypsin, Lancet 323 (1984) 169–170.
[6] O.H. Kang, H.J. Jeong, D.K. Kim, S.C. Choi, T.H. Kim, Y.H. Nah, H.M. Kim, Y.M. Lee, Trypsin induces tumour necrosis factor-α secretion from a human leukemic mast cell line, Cell Biochem. Funct. 21 (2003) 161–167.
[7] K. Ochiai, K. Kaneko, M. Kitagawa, H. Ando, T. Hayakawa, Activated pancreatic enzyme and pancreatic stone protein (PSP/reg) in bile of patients with pancreaticobiliary maljunction/choledochal cysts, Dig. Dis. Sci. 49 (2004) 1953–1956.
[8] E.J. Bures, C.C. Siska, A.A. Raibekas, High-performance liquid chromatography-based protease detection at the picogram level, Anal. Biochem. 326 (2004) 276–277.
[9] M.A. Seia, P.W. Stege, S.V. Pereira, I.E. De Vito, J. Raba, G.A. Messina, Silica nanoparticle-based microfluidic immunosensor with laser-induced fluorescence detection for the quantification of immunoreactive trypsin, Anal. Biochem. 463 (2014) 31–37.
[10] M.M. Dong, H.L. Qi, S.G. Ding, M. Li, Electrochemical determination of trypsin using a heptapeptide substrate self-assembled on a gold electrode, Microchim. Acta 182 (2015) 43–49.
[11] X. Liu, Y. Li, L. Jia, S. Chen, Y.H. Shen, Ultrasensitive fluorescent detection of trypsin on the basis of surfactant–protamine assembly with tunable emission wavelength, RSC Adv. 6 (2016) 93551–93557.
[12] A.D. Shao, Z.Q. Guo, S.J. Zhu, S.Q. Zhu, P. Shi, H. Tian, W.H. Zhu, Insight into aggregation-induced emission characteristics of red-emissive quinoline-malononitrile by cell tracking and real-time trypsin detection, Chem. Sci. 5 (2014) 1383–1389.
[13] Y.Y. Lin, R. Chapman, M.M. Stevens, Label-free multimodal protease detection based on protein/perylene dye coassembly and enzyme-triggered disassembly, Anal. Chem. 86 (2014) 6410–6417.
[14] W.Z. Zhang, P. Zhang, S.Z. Zhang, C.Q. Zhu, Label-free and real-time monitoring of trypsin activity in living cells by quantum-dot-based fluorescent sensors, Anal. Meth. 6 (2014) 2499–2505.
[15] C.Y. Poon, Q.H. Li, J.L. Zhang, Z.P. Li, C. Dong, A.W. Lee, W. Chan, H. Li, FRET-based modified graphene quantum dots for direct trypsin quantification in urine, Anal. Chim. Acta 917 (2016) 64–70.
[16] L.Y. Chen, C.W. Wang, Z.Q. Yuan, H.T. Chang, Fluorescent gold nanoclusters: recent advances in sensing and imaging, Anal. Chem. 87 (2014) 216–229.
[17] M.L. Cui, Y. Zhao, Q.J. Song, Synthesis, optical properties and applications of ultra-small luminescent gold nanoclusters, Trends Anal. Chem. 57 (2014) 73–82.
[18] J.P. Xie, Y.G. Zheng, J.Y. Ying, Protein-directed synthesis of highly fluorescent gold nanoclusters, J. Am. Chem. Soc. 131 (2009) 888–889.
[19] Y. Liu, P. Dong, Q. Jiang, F. Wang, D. Pang, X. Liu, Assembly-enhanced fluorescence from metal nanoclusters and quantum dots for highly sensitive biosensing, Sens. Actuators B 279 (2019) 334–341.
[20] R.P. Li, P.P. Xu, J. Fan, J.W. Di, Y.F. Tu, J.L. Yan, Sensitive iodate sensor based on fluorescence quenching of gold nanocluster, Anal. Chim. Acta 827 (2014) 80–85.
[21] X. Yan, H.X. Li, B.C. Cao, Z.Y. Ding, X.G. Su, A highly sensitive dual-readout assay based on gold nanoclusters for folic acid detection, Microchim. Acta 182 (2015) 1281–1288.
[22] M. Santhosh, S.R. Chinnadayyala, A. Kakoti, P. Goswami, Selective and sensitive detection of free bilirubin in blood serum using human serum albumin stabilized gold nanoclusters as fluorometric and colorimetric probe, Biosens. Bioelectron. 59 (2014) 370–376.
[23] M. Santhosh, S.R. Chinnadayyala, N.K. Singh, P. Goswami, Human serum albumin-stabilized gold nanoclusters act as an electron transfer bridge supporting specific electrocatalysis of bilirubin useful for biosensing applications, Bioelectrochemistry 111 (2016) 7–14.
[24] H.C. Dai, Y. Shi, Y.L. Wang, Y.J. Sun, J.T. Hu, P.J. Ni, Z. Li, Label-free turn-on fluorescent detection of melamine based on the anti-quenching ability of Hg^{2+} to gold nanoclusters, Biosen. Bioelectron. 53 (2014) 76–81.
[25] Z.T. Luo, X. Yuan, Y. Yu, Q.B. Zhang, D.T. Leong, J.Y. Lee, J.P. Xie, From aggregation-induced emission of Au (I)–thiolate complexes to ultrabright Au (0)@Au (I)–thiolate core–shell nanoclusters, J. Am. Chem. Soc. 134 (2012) 16662–16670.
[26] X. Li, S.J. Zhu, B. Xu, K. Ma, J.H. Zhang, B. Yang, W.J. Tian, Self-assembled graphene quantum dots induced by cytochrome c: a novel biosensor for trypsin with remarkable fluorescence enhancement, Nanoscale 5 (2013) 7776–7779.
[27] P. Wu, T. Zhao, J.Y. Zhang, L. Wu, X.D. Hou, Analyte-activable probe for protease based on cytochrome C-capped Mn: ZnS quantum dots, Anal. Chem. 86 (2014) 10078–10083.
[28] H. Lin, L.J. Li, C.Y. Lei, X.H. Xu, Z. Nie, M.L. Guo, Y. Huang, S.Z. Yao, Immune-independent and label-free fluorescent assay for Cystatin C detection based on protein-stabilized Au nanoclusters, Biosens. Bioelectron. 41 (2013) 256–261.
[29] X. Yan, Y. Song, C.Z. Zhu, J.H. Song, D. Du, X.G. Su, Y.H. Lin, Graphene quantum dot-MnO_2nanosheet based optical sensing platform: a sensitive fluorescence "Turn Off-On" nanosensor for glutathione detection and intracellular imaging, ACS Appl. Mater. Interfaces 8 (2016) 21990–21996.
[30] J. Xu, K. Haupt, B.T.S. Bui, Core-shell molecularly imprinted polymer nanoparticles as synthetic antibodies in a sandwich fluoroimmunoassay for trypsin determination in human serum, ACS Appl. Mater. Interfaces 9 (2017) 24476–24483.
[31] L. Su, T. Shu, Z. Wang, J.Y. Cheng, F. Xue, C.Z. Li, X.J. Zhang, Immobilization of

bovine serum albumin-protected gold nanoclusters by using polyelectrolytes of opposite charges for the development of the reusable fluorescent Cu^{2+}-sensor, Biosens. Bioelectron. 44 (2013) 16–20.
[32] Y.Q. Cai, L. Yan, G.Y. Liu, H.Y. Yuan, D. Xiao, In-situ synthesis of fluorescent gold nanoclusters with electrospun fibrous membrane and application on Hg (II) sensing, Biosens. Bioelectron. 41 (2013) 875–879A..
[33] A. Ghosh, V. Jeseentharani, M.A. Ganayee, R.G. Hemalatha, K. Chaudhari, C. Vijayan, T. Pradeep, Approaching sensitivity of tens of ions using atomically precise cluster-nanofiber composites, Anal. Chem. 86 (2014) 10996–11001.
[34] Y. Jia, W. Zheng, X. Zhao, J. Zhang, W. Chen, X. Jiang, Mixing-to-answer iodide sensing with commercial chemicals, Anal. Chem. 90 (2018) 8276–8282.
[35] X. Yan, H.X. Li, W.S. Zheng, X.G. Su, Visual and fluorescent detection of tyrosinase activity by using a dual-emission ratiometric fluorescence probe, Anal. Chem. 87 (2015) 8904–8909.
[36] A.C. Fu, Y. Hu, Z.H. Zhao, R.L. Su, Y.L. Song, D. Zhu, Functionalized paper microzone plate for colorimetry and up-conversion fluorescence dual-mode detection of telomerase based on elongation and capturing amplification, Sens. Actuators B 259 (2018) 642–649.
[37] D.M. Cate, J.A. Adkins, J. Mettakoonpitak, C.S. Henry, Recent developments in paper-based microfluidic devices, Anal. Chem. 87 (2015) 19–41.
[38] Han, L. Xiong, S. Hao, Y. Yang, X. Li, G. Fang, J. Liu, Y. Pei, S. Wang, Anal. Chem. 90 (2018) 9060–9067.

Hongxia Li received her M.S. degree in 2013 from Nanjing Agricultural University. and received her Ph.D. degree in 2016 at Jilin University. Since then, she did postdoctoral work with Prof. Geyu Lu. Currently, her research interests mainly focus on the development of the functional nanomaterials for chem/bio sensors.

Mingming Yang Currently, she is studying for her Ph.D. degree in College of Plant Protection, Nanjing Agricultural University. Her research interests mainly focus on the development of the functional nanomaterials for chem/bio sensors.

Deshuai Kong received her B. Eng. degree in department of Microelectronics science and engineering, Jilin University in 2018. Now, she is about to assiduously study for her M.S. degree in College of Electronic Science and Engineering, Jilin University, China. Currently, her research interests mainly focus on the application of gold nanoclusters.

Rui Jin received her M.S. degree in 2016 from College of Chemistry, Jilin University, China. Currently, she is studying for her Ph.D. degree in College of Electronic Science and Engineering, Jilin University. Her research interests mainly focus on the development of the functional nanomaterials for chem/bio sensors.

Xu Zhao received the B. Eng. degree in department of electronic sciences and technology, Jilin University in 2016. Now, he is studying for his MS degree in College of Electronic Science and Engineering, Jilin University, China. Currently, his research interests mainly focus on the development of the functional nanomaterials for chem/bio sensors.

Fangmeng Liu received his PhD degree in 2017 from College of Electronic Science and Engineering, Jilin University, China. Now he is a lecturer of Jilin University, China. His current research interests include the application of functional materials and development of solid state electrolyte gas sensor and flexible device.

Xu Yan received his M.S. degree in 2013 from Nanjing Agricultural University. He joined the group of Prof. Xingguang Su at Jilin University and received his Ph.D. degree in June 2017. Since then, he did postdoctoral work with Prof. Geyu Lu and Prof. Junqiu Liu. Currently, his research interests mainly focus on the development of the functional nanomaterials for chem/bio sensors.

Yuehe Lin is a professor at Washington State University and a Laboratory Fellow at Pacific Northwest National Laboratory. His research interests include electrochemistry, bioanalytical chemistry, chemical sensors and biosensors, fuel cells and batteries, material synthesis and applications. He is a fellow of the American Association of the Advancement of Science (AAAS), the Royal Society of Chemistry of the UK, and the American Institute for Medical and Biological Engineering (AIMBE).

Geyu Lu received the B. Sci. degree in electronic sciences in 1985 and the M. Sci. degree in 1988 from Jilin University in China and the Dr. Eng. degree in 1998 from Kyushu University in Japan. Now he is a professor of Jilin University, China. His current research interests include the development of chemical sensors and the application of the function materials.